University of Wollongong

Research Online

Faculty of Engineering - Papers (Archive)

Faculty of Engineering and Information Sciences

1-1-2009

Effects of cobalt doping and phase diagrams of LFe1-xCox AsO (L=La and Sm)

Cao Wang
Zhejiang University, caow@uow.edu.au

Y K. Li
Zhejiang University

Z W. Zhu
Zhejiang University

S Jiang
Zhejiang University

X Lin
Zhejiang University

See next page for additional authors

Follow this and additional works at: https://ro.uow.edu.au/engpapers

Part of the Engineering Commons

https://ro.uow.edu.au/engpapers/5143

Authors

Cao Wang, Y K. Li, Z W. Zhu, S Jiang, X Lin, Y K. Luo, S Chi, L J. Li, Z Ren, M He, H Chen, Y T. Wang, Q Tao, G H. Cao, and Z A. Xu

Effects of cobalt doping and phase diagrams of LFe$_{1-x}$Co$_x$AsO (L=La and Sm)

C. Wang, Y. K. Li, Z. W. Zhu, S. Jiang, X. Lin, Y. K. Luo, S. Chi, L. J. Li, Z. Ren, M. He, H. Chen, Y. T. Wang, Q. Tao, G. H. Cao,[*] and Z. A. Xu[†]

Department of Physics, Zhejiang University, Hangzhou 310027, People's Republic of China
(Received 31 August 2008; published 20 February 2009)

The superconducting phase diagrams have been established by the measurements of electrical resistivity, magnetic susceptibility, and thermopower in cobalt-doped LFeAsO (L=La and Sm) systems. It is shown that the antiferromagnetic spin-density-wave order in the parent compounds is rapidly suppressed by Co doping, and superconductivity emerges at $x=0.025$ and 0.05 in LaFe$_{1-x}$Co$_x$AsO and SmFe$_{1-x}$Co$_x$AsO, respectively. The $T_c(x)$ curves of both systems are domelike, with a maximum T_c of 13 K at $x=0.075$ in LaFe$_{1-x}$Co$_x$AsO and 17.2 K at $x=0.1$ in SmFe$_{1-x}$Co$_x$AsO. Thermopower measurement shows dominant electron-type transport for the Co-doped samples, in accordance with itinerant character of Co $3d$ electrons. We found a close correlation between T_c and the abnormally enhanced part of normal-state thermopower. The occurrence of superconductivity via the Fe-site doping in the iron-based oxyarsenide contrasts sharply with the destruction of superconductivity by the Cu-site (within CuO$_2$ planes) doping in high-temperature superconducting cuprates.

I. INTRODUCTION

Recent discovery of superconductivity (SC) at 26 K in LaFeAsO$_{1-x}$F$_x$ (Ref. 1) has opened a new chapter in superconductivity research. The superconductivity was induced by partial substitution of O^{2-} with F$^-$ in the parent compound LaFeAsO whose crystal structure consists of insulating [La$_2$O$_2$]$^{2+}$ layers and conducting [Fe$_2$As$_2$]$^{2-}$ layers.[2] Following this discovery, the superconducting transition temperature T_c over 40 K was realized in LFeAsO$_{1-x}$F$_x$ (L=lanthanides) (Refs. 3–5) and oxygen-deficient LFeAsO$_{1-\delta}$.[6,7] Through an alternative chemical doping of thorium for gadolinium, T_c has achieved 56 K in Gd$_{0.8}$Th$_{0.2}$FeAsO.[8] The above substitutions introduce extra positive charges in the insulating L_2O$_2$ layers, and extra electrons are produced onto the Fe$_2$As$_2$ layers as a result of charge neutrality. The occurrence of superconductivity in this sense is rather similar to cuprate superconductors in which superconductivity appears when appropriate amounts of charge carriers are transferred into the CuO$_2$ planes by chemical doping at "charge reservoir layers."[9]

However, band-structure calculations and theoretical analysis reveal itinerant character of Fe $3d$ electrons in the iron-based oxyarsenides.[10–12] The calculated electron density of states (DOS) for LaMAsO (M=Mn, Fe, Co, and Ni) (Ref. 13) shows that the main feature of total DOS remains unchanged, except that Fermi level shifts toward the top of valence band with band filling (adding electrons) one by one from M=Mn, Fe, Co, to Ni. According to this calculation, substitution of cobalt for iron is expected to induce electrons directly onto FeAs layers. On the other hand, Co-doping at Fe site induces disorder in FeAs layers, which is not beneficial to superconductivity. Therefore, it is of great interest to explore the cobalt-doping effect in LFeAsO systems.

Sefat *et al.*[14] first reported the synthesis and basic characterization of LaFe$_{1-x}$Co$_x$AsO. They observed superconductivity with $x=0.05$, 0.11, and 0.15. We also independently found that Co doping induces superconductivity in LaFeAsO system.[15] The superconducting phase diagram has been ob-

tained by using a series of high-quality samples with $x=0$, 0.01, 0.025, 0.05, 0.075, 0.1, 0.125, 0.15, and 0.2. Our subsequent systematic work on SmFe$_{1-x}$Co$_x$AsO further confirms that Co doping is effective to induce superconductivity in the iron arsenide system. The maximum T_c achieves 17.2 K at $x=0.10$. We found a close correlation between T_c and the abnormally enhanced part of normal-state thermopower, implying the importance of spin fluctuations for the superconducting mechanism in the oxyarsenide. It is noted[15] that superconductivity in SmFe$_{1-x}$Co$_x$AsO was also independently reported by Qi *et al.*,[16] who observed a relatively low T_c^{mid} of 14.2 K for $x=0.10$.

II. EXPERIMENTAL

Polycrystalline samples of LFe$_{1-x}$Co$_x$AsO (L=La and Sm) were synthesized by solid-state reaction in vacuum using powders of LaAs, SmAs, La$_2$O$_3$, Sm$_2$O$_3$, FeAs, Fe$_2$As, and Co$_3$O$_4$. LaAs and SmAs were presynthesized by reacting stoichiometric La pieces and As powders in evacuated quartz tubes at 1173–1223 K for 24 h. FeAs and Fe$_2$As were prepared by reacting stoichiometric Fe powders and As powders at 873 K for 10 h, respectively. Co$_3$O$_4$ and La$_2$O$_3$ were dried by firing in air at 773 and 1173 K, respectively, for 24 h before using. All the starting materials are with high purity ($\geq 99.9\%$). The powders of these intermediate materials were weighed according to the stoichiometric ratios of LaFe$_{1-x}$Co$_x$AsO ($x=0$, 0.01, 0.025, 0.05, 0.075, 0.1, 0.125, 0.15, and 0.2) and SmFe$_{1-x}$Co$_x$AsO ($x=0$, 0.01, 0.025, 0.05, 0.075, 0.1, 0.125, 0.15, 0.175, 0.2, 0.225, 0.25, and 0.3) and thoroughly mixed in an agate mortar and pressed into pellets under a pressure of 2000 kg/cm^2, all operating in a glove box filled with high-purity argon. The pellets were sealed in evacuated quartz tubes, then heated uniformly at 1433 K for 40 h, and finally furnace cooled to room temperature.

Powder x-ray diffraction (XRD) was performed at room temperature using a D/Max-rA diffractometer with Cu K$_\alpha$ radiation and a graphite monochromator. The XRD diffractometer system was calibrated using standard Si powders.
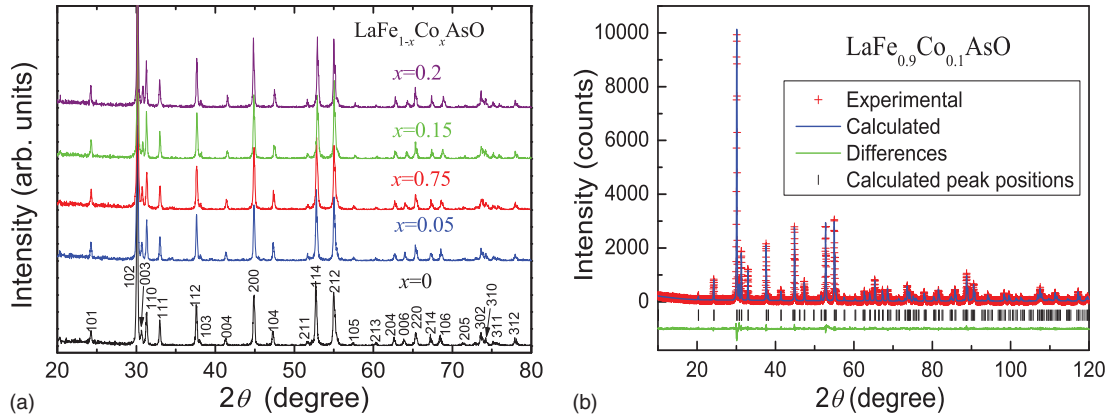
FIG. 1. (Color online) (a) Powder x-ray diffraction patterns of LaFe$_{1-x}$Co$_x$AsO samples. (b) An example of Rietveld refinement profile for $x=0.1$.

Lattice parameters were calculated by a least-squares fit using at least 20 XRD peaks in the range of $20° \leq 2\theta \leq 80°$. The errors were estimated as three times of the standard deviations of the fit. Crystal structure parameters were obtained by Rietveld refinement using the step-scan XRD data with $10° \leq 2\theta \leq 120°$ for LaFe$_{1-x}$Co$_x$AsO. The refined lattice constants are essentially the same with those of least-squares fit within the scope of estimated errors. The typical R values of the refinements are: $R_F \sim 3\%$, $R_B \sim 4\%$, and $R_{wp} \sim 13\%$. The goodness-of-fit parameter $S = R_{wp}/R_{exp} \sim 1.5$, indicating good reliability of the refinement.[17] The errors of the refinement for oxygen occupancy, taken as twice of the estimated standard deviations, are 0.03.

The electrical resistivity was measured with a standard four-terminal method. Samples were cut into a thin bar with typical size of $4 \times 2 \times 0.5$ mm^3. Gold wires were attached onto the samples' abraded surface with silver paint. The size of the contact pads leads to total uncertainty in the absolute values of resistivity of 10%. The electrical resistance was measured using a steady current of 5 mA, after checking the linear I-V characteristic. Thermopower measurements were carried out on a Quantum Design physical property measurement system (PPMS-9) by a steady-state technique with a temperature gradient of 1–2 K/cm. Temperature dependence of magnetization was measured on a Quantum Design magnetic property measurement system (MPMS-5). For the measurement of the superconducting transitions, both the zero-field-cooling and field-cooling protocols were employed under the magnetic field of 10 Oe.

III. RESULTS AND DISCUSSION

A. Superconductivity in LaFe$_{1-x}$Co$_x$AsO

Figure 1(a) shows the XRD patterns of the synthesized LaFe$_{1-x}$Co$_x$AsO samples. The XRD peaks can be well indexed based on a tetragonal cell of LaFeAsO,[2] indicating that the samples are almost single phase. Only trace amounts of impurities (less than 2%, according to the relative intensities of their strongest XRD reflections) of FeAs and/or La$_2$O$_3$ can be identified. The good phase purity holds for all the Co-doping levels, suggesting that Co atoms are mostly incorporated into the lattice. An example of Rietveld refinement based on ZrCuSiAs-type structure is given in Fig. 1(b). The calculated intensities match very well with the experimental data.

Figure 2(a) plots the lattice parameters (from the Rietveld refinements) as a function of Co content. With increasing Co content, the a axis remains nearly unchanged while the c axis shrinks significantly. Thus the cell volume decreases almost
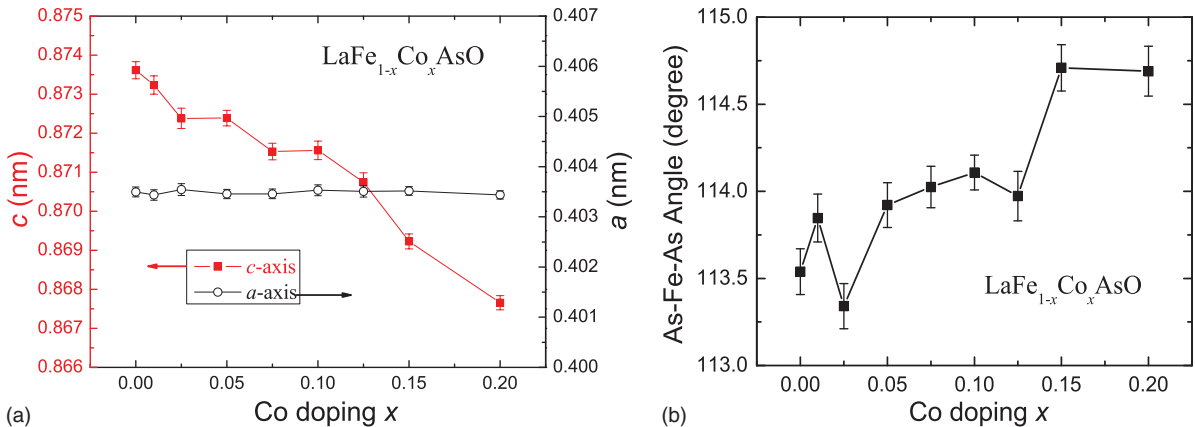

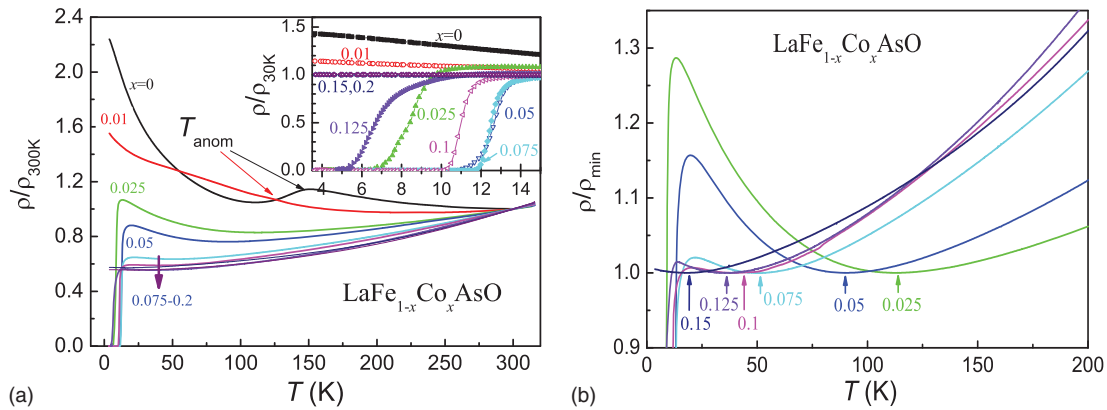FIG. 2. (Color online) (a) Lattice parameters and (b) angles of As-Fe-As as a function of Co content in LaFe$_{1-x}$Co$_x$AsO.

FIG. 3. (Color online) Temperature dependence of electrical resistivity, normalized to (a) $\rho_{300\ K}$ and to (b) ρ_{min}, of LaFe$_{1-x}$Co$_x$AsO polycrystalline samples. The inset of panel (a) is an expanded plot, showing the superconducting transitions. The arrows in panel (b) mark the positions of T_{min}, where the resistivity exhibits a minimum, for various doping levels.

linearly, which is related to the smaller Co^{2+} ions (as compared with Fe^{2+} ions). This result is consistent with other related reports.[14] The change in lattice parameters indicates that Co was successfully doped into the lattice, according to Vegard's law. The shrinkage of c axis suggests the strengthening of interlayer Coulomb attraction, implying the increase in density of negative charge in FeAs layers by the Co doping.

The oxygen content in LaFe$_{1-x}$Co$_x$AsO is an important issue in present study because oxygen deficiency itself might induce superconductivity. By high-pressure synthesis, superconductivity was indeed observed in oxygen-deficient LFeAsO$_{1-\delta}$.[6,7] It has also been reported that superconductivity was induced by oxygen deficiency in Sr-doped LaFeAsO via annealing in vaccum.[18] We note that all the reported superconductors showed a *remarkable* (0.3%~0.6%) decrease in a axis owing to the oxygen deficiency. However, the present LaFe$_{1-x}$Co$_x$AsO samples show no obvious change ($\pm0.03\%$) in a axis, suggesting no significant oxygen deficiency. We also refined the oxygen occupancy by the Rietveld analysis. The result shows that the oxygen content is 0.99 ± 0.03, independent of Co doping. So, even if there exists a small level of oxygen deficiency, the *doping-independent* oxygen deficiency cannot account for the superconducting phase diagram shown below.

In the iron-based arsenides, the structural features of FeAs layers were linked with superconductivity. It was revealed that T_c increases with decrease in the bond angle of As-Fe-As.[19,20] The maximum T_c correspond to the regular tetrahedron of FeAs$_4$ with the bond angle at 109.5°. Figure 2(b) shows the As-Fe-As angle as a function of Co doping in LaFe$_{1-x}$Co$_x$AsO. The As-Fe-As angle of the undoped LaFeAsO is 113.5°, consistent with the previous report.[20] With increasing Co content, the angle tends to increase. The angles for the superconducting samples (see below) are about 114°, which is obviously larger than that of LaFeAsO$_{1-\delta}$.[20] The relatively large As-Fe-As angles may account for the relatively low T_c values in LaFe$_{1-x}$Co$_x$AsO.

Figure 3 shows the temperature dependence of electrical resistivity (ρ) of LaFe$_{1-x}$Co$_x$AsO. For the parent compound, an anomaly characterized by a drop in ρ was observed below

150 K, consistent with the previous reports.[1,11] However, the resistivity shows a more pronounced upturn at lower temperatures. Neutron-diffraction study[21] indicated a structural phase transition at 155 K followed by an antiferromagnetic (AFM) spin-density-wave (SDW) transition at 137 K in LaFeAsO. The drop in ρ (and also magnetic susceptibility, χ, shown in the inset of Fig. 4) happens at the structural transition temperature,[22,23] which was interpreted as the result of incipient magnetic order.[24] Upon doping with Co, the anomaly temperature T_{anom} was suppressed to 135 K for x =0.01, and the anomaly became very weak (only a small kink in ρ appeared at the T_{anom}). For $0.025 < x < 0.125$, the resistivity anomaly disappears; instead, a resistivity minimum shows up at T_{min} depending on the Co-doping levels. Superconductivity emerges at lower temperatures. The inset of Fig. 3(a) clearly shows that the superconducting transition temperature T_c^{mid}, defined as the midpoint in the resistive transition, is from 7 to 13 K. The superconducting transition width is only $1\sim2$ K. The samples of x=0.15 and 0.2 show no sign of superconducting transition above 3 K, the lowest temperature achieved in our resistivity measurement.
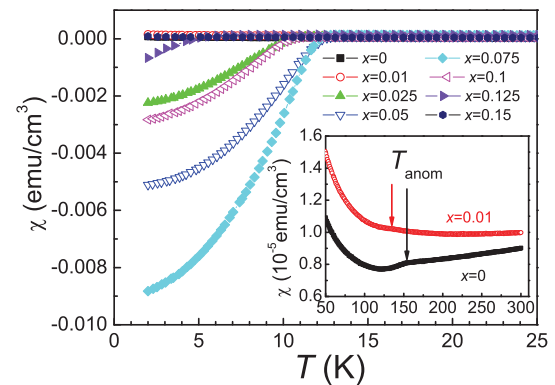

FIG. 4. (Color online) Magnetic susceptibility (χ) of LaFe$_{1-x}$Co$_x$AsO samples. Field-cooling protocols were used under the field of 10 Oe. The inset shows the $\chi(T)$ data for the samples of x=0 and 0.01, measured under the magnetic field of 1000 Oe. A drop/kink in χ can be found at 150 and 135 K for x=0 and 0.01, respectively.
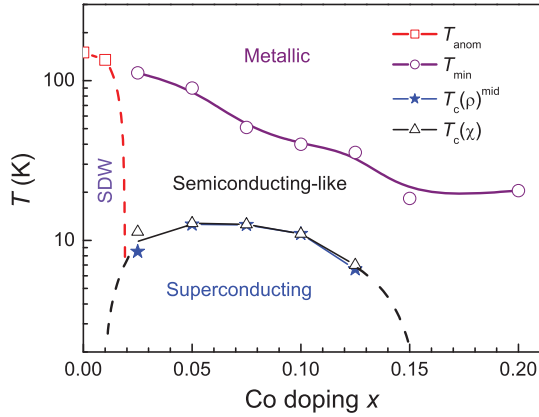
FIG. 5. (Color online) The electronic phase diagram of LaFe$_{1-x}$Co$_x$AsO. T_{anom} denotes the resistivity anomaly temperature. T_{min} separates the metallic and semiconductinglike regions in the normal state of the superconductors. The dashed lines are based on the measurement limit. Note that the vertical axis is in logarithmic scale.

TABLE I. Comparison of electronic phase diagrams in LFeAsO$_{1-x}$F$_x$ (Ref. 26) and LaFe$_{1-x}$Co$_x$AsO (present work). $T_{c,max}$ denotes the maximum T_c at optimal doping level x_{opt}.

System	LaFeAsO$_{1-x}$F$_x$	LaFe$_{1-x}$Co$_x$AsO
SDW region	$0 \leq x \leq 0.04$	$0 \leq x < 0.025$
SC region	$0.04 < x \leq 0.2$ [a]	$0.025 \leq x \leq 0.125$
$T_{c,max}$ (K)	26	13
x_{opt}	~ 0.1	~ 0.06
$\rho(T)$ above T_c at x_{opt}	metallic	semiconductinglike

[a]The superconducting region is limited by the solubility limit of F doping. In fact, $T_c \sim 10$ K for $x=0.2$.

It is noted that the normal-state resistivity exhibits an upturn above T_c, as can be clearly seen in Fig. 3(b). At first glance, Anderson localization seems to account for the resistivity upturn at low temperatures. However, such a disorder effect would lead to a pronounced resistivity upturn with increasing Co doping, contradicting the experimental observations. Similarly, attempt to interpret the resistivity minimum in terms of conventional Kondo effect is unsuccessful either, if the doped Co is regarded as magnetic impurity. Further study is needed to clarify this issue.

Figure 4 shows the magnetic susceptibility measurement result. Samples with $0.025 \leq x \leq 0.125$ show strong diamagnetic signal. The magnetic expelling (Meissner effect) fraction and magnetic shielding fraction of the sample of $x=0.075$ are estimated to be 11% and 30%, respectively, confirming bulk superconductivity. For samples of $x=0$, 0.01, and 0.15, no superconductivity transition was observed down to 2 K. Although the susceptibility shows Curie-Weiss-type upturn at low temperatures (see the inset of Fig. 4), the fitted effective moments are very small, x independent and sample dependent. Thus the Curie-Weiss-type behavior is likely due to an extrinsic origin (such as defects and trace impurities). The absence of appreciable intrinsic localized moments in LaFe$_{1-x}$Co$_x$AsO up to $x=0.2$ suggests that the electrons of the doped Co is basically itinerant because the ionic Co^{2+} and Co^{3+} would definitely have localized moments under the tetrahedron crystal field irrespective of high-spin and low-spin states.

The electronic phase diagram for LaFe$_{1-x}$Co$_x$AsO was thus obtained from the above experimental data, as depicted in Fig. 5. The phase region of the SDW (or incipient SDW) is very narrow. Co doping by 2.5% completely destroys the SDW order, and superconductivity emerges. In the superconducting regime with $0.025 \leq x \leq 0.125$, one sees a domelike $T_c(x)$ curve. Though the normal state shows metallic conduction at high temperatures, semiconductinglike behavior is always observed above T_c. It is noted here that the borderline between metallic and semiconductinglike regions is not well

established because polycrystalline samples were employed. For the higher Co-doping levels of $x \geq 0.15$, superconductivity no longer survives. It was reported that the sample of $x =0.15$ shows superconductivity at 6.0 K.[14] This discrepancy may be due to the deviation of chemical composition when the sample contains significant impurities. Further Co doping is also of interest because the other end member LaCoAsO was an itinerant ferromagnetic metal.[25]

The present Co-doped LaFeAsO system shows both similarities and differences in comparison with the phase diagram of F-doped LaFeAsO.[1,11,26] On one hand, the SDW state in LaFeAsO is suppressed or destroyed, and superconductivity occurs with a domelike $T_c(x)$ upon electron doping in both systems. On the other hand, however, there are some differences as listed in Table I. Here we note the following points: (1) Co doping destroys the AFM SDW order more strongly; superconductivity appears at surprisingly small doping level. (2) The maximum T_c is significantly lowered in Co-doped system. (3) The optimal doping level is distinctly lower and the superconducting region is narrower in LaFe$_{1-x}$Co$_x$AsO system. (4) The normal state of LaFe$_{1-x}$Co$_x$AsO system shows semiconductinglike behavior above T_c.

The first issue can be qualitatively understood in terms of the variation in exchange interactions. According to the theoretical studies,[27–29] the AFM order in the parent compound originates from the competing nearest-neighbor and next-nearest-neighbor superexchange interactions, bridged by As $4p$ orbitals. Both interactions are antiferromagnetic, which gives rise to a frustrated magnetic ground state (Fig. 6). Upon doping Co into the Fe site, the original AFM superexchange interactions may be changed into a double exchange between Co and Fe atoms, which obviously destroys the stripelike AFM order. Different number of $3d$ electrons at Fe^{2+} and Co^{2+} validates the double exchange in the form of Fe$^{2+}3d \frown$As$^{3-}4p \frown$Co$^{2+}3d$, analogous to the classic double exchange interaction in perovskite-type manganites.[30] The appearance of superconductivity at $x \sim 0.025$ suggests that the suppression of the SDW order by the Fe-site doping plays an important role to induce superconductivity.

The lowered T_c in LaFe$_{1-x}$Co$_x$AsO system seems to be related to the disorder effect within (Fe/Co)As layers. Generally, impurity-induced disorder may suppress superconductivity. The insensitivity of superconductivity to a large degree of Fe/Co disorder in FeAs layers is consistent with itinerant character of the $3d$ electrons in the iron-based oxyarsenides
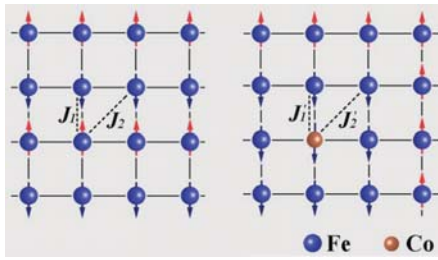
FIG. 6. (Color online) Destruction of antiferromagnetism in Fe planes by Co doping. Left: the nearest-neighbor (J_1) and next-nearest-neighbor (J_2) superexchange interactions result in a stripe-like AFM order in Fe planes when $J_2 > 2J_1 > 0$. Right: the adjacent interactions between Fe and Co become ferromagnetic ($J_2' < 0$) due to a double exchange, which easily destroys the original frustrated AFM order.

because the itinerant electrons may smear out the disorder potentials to some extent. Apart from the possible disorder effect, the lowered $T_{c,max}$ may arise from a structural reason since the related bond angle and/or bond length affect the effective bandwidth in the present materials.[19] As mentioned above, the Co-doped system shows relatively large As-Fe-As angle (about 114°). The angles are obviously larger than those of LaFeAsO$_{1-x}$F$_x$ (e.g., the As-Fe-As angle is calculated to be 112.8° for $x=0.14$ using the structural data of Ref. 23), which may lead to the lowered $T_{c,max}$.

B. Superconductivity in SmFe$_{1-x}$Co$_x$AsO

Figure 7(a) shows the representative XRD patterns of the SmFe$_{1-x}$Co$_x$AsO samples. The diffraction peaks of all the samples can be well indexed based on a tetragonal cell of ZrCuSiAs-type structure, which indicates that the samples are all nearly pure phase. Figure 7(b) shows the variations in refined lattice parameters with Co content. Similar to the case of LaFe$_{1-x}$Co$_x$AsO, Co doping causes the shrinkage of the c axis significantly, while the a axis remains nearly unchanged.

Figure 8 shows the temperature dependence of electrical resistivity of SmFe$_{1-x}$Co$_x$AsO samples in the temperature range of 3–300 K. The inset shows an enlarged plot of ρ versus T for the low temperatures. For the undoped parent compound, a clear drop in the resistivity is observed below about 140 K just as in the case of LaFeAsO,[1] which has been ascribed to a structural phase transition and antiferromagnetic spin-density-wave (SDW) transition.[21] This anomalous temperature T_{anom}, which is defined as the peak position in the temperature dependence of the derivative of resistivity, decreases from 137 K for $x=0$ to 124 and 93 K for $x=0.01$ and 0.025, respectively. For $x=0.05$, such an anomalous change in resistivity almost disappears, and only a tiny kink around 45 K can be distinguished. Within the doping range of $0.05 \leq x \leq 0.20$, superconducting transition can be observed at low temperatures. Meanwhile, the resistivity anomaly disappears completely for $x > 0.05$. This means that the superconductivity occurs wherefrom the suppression of SDW order takes place. T_c^{mid} reaches a maximum of 17.2 K at the "optimally doped" level $x=0.1$, which is distinctly
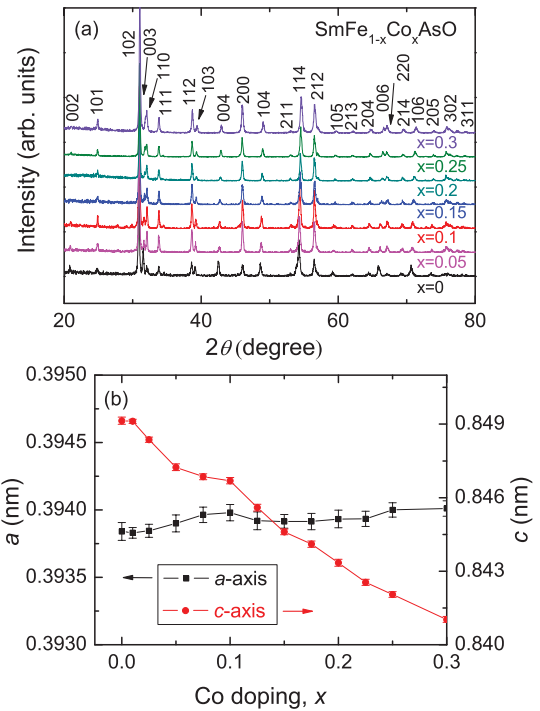
higher than the reported value of 14.2 K.[16] This maximum of T_c^{mid} is larger than that of LaFe$_{1-x}$Co$_x$AsO. The volume fraction of magnetic shielding is over 60% for the "optimally" doped sample estimated according to its magnetic susceptibility (not shown here). Furthermore, the "superconducting window" is in the doping range of $0.05 \leq x \leq 0.20$, which is also larger compared to the superconducting window ($0.025 \leq x \leq 0.125$) for LaFe$_{1-x}$Co$_x$AsO system.

Similar to LaFe$_{1-x}$Co$_x$AsO, the resistivity changes from metallic into semiconductorlike as $T < T_{min}$ in

FIG. 7. (Color online) Structural characterization of SmFe$_{1-x}$Co$_x$AsO samples. (a) Powder x-ray diffraction patterns of representative SmFe$_{1-x}$Co$_x$AsO samples. (b) Lattice parameters as a function of Co content.

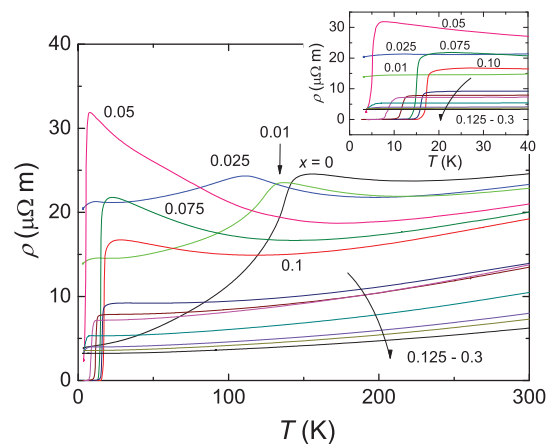FIG. 8. (Color online) Temperature dependence of resistivity (ρ) for the SmFe$_{1-x}$Co$_x$AsO samples. Inset: the enlarged plot of ρ versus T for low temperatures, showing the superconducting transitions.
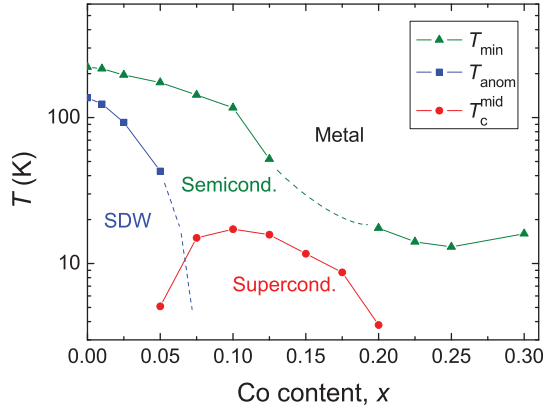
FIG. 9. (Color online) The electronic phase diagram for SmFe$_{1-x}$Co$_x$AsO. In the dashed line of T_{min}, the resistivity minimum was absent because of the onset of superconductivity. Note that the vertical axis is in logarithmic scale.

FIG. 10. (Color online) Temperature dependence of thermopower (S) in LaFe$_{1-x}$Co$_x$AsO. The inset of panel (a) is an expanded plot, showing the superconducting transitions.

SmFe$_{1-x}$Co$_x$AsO; i.e., there exists a crossover from metal into insulator as T decreases. However, such a resistivity upturn disappears in the doping regime of $0.15 \leq x \leq 0.175$. We suggest that this upturn could be hidden in the strong superconducting fluctuations as T_c^{onset}, the onset point in the resistive transition, is quite high in this regime. Meanwhile the room-temperature resistivity shows a monotonous decrease with increasing x. In the region of large Co-doping level ($x > 0.15$), the temperature dependence of resistivity follows a power law for temperature range $T > T_{min}$, i.e., $\rho \propto T^n$. The index n is about 1.65 for $x = 0.25$. The system becomes more metallic with increasing Co content.

Based on the above resistivity data, an electronic phase diagram for SmFe$_{1-x}$Co$_x$AsO was thus established, as shown in Fig. 9. The phase region of the SDW state is quite narrow. 5% Co doping almost destroys the SDW order, and superconductivity emerges. In the range of $0.05 \leq x \leq 0.20$, a domelike $T_c(x)$ curve is observed, similar to that of LaFe$_{1-x}$Co$_x$AsO. However, the details of the domes are different. Not only is the value of $T_{c,max}$ distinctly larger but also the superconducting window shifts to higher doping levels in SmFe$_{1-x}$Co$_x$AsO. Thus, it is difficult to make a scaling for the $T_c(x)$ data of the two systems. The normal state shows metallic conduction at high temperatures, but it changes into semiconductinglike before superconducting transition. For the higher Co-doping levels ($x \geq 0.20$), superconductivity is quenched though the resistivity becomes more metallic. It is noted that complete replacement of Fe by Co is possible, but whether SmCoAsO is an itinerant ferromagnetic metal like LaCoAsO (Ref. 25) needs to be clarified.

C. Thermopower

Figure 10 shows the temperature dependence of thermopower (S) in LaFe$_{1-x}$Co$_x$AsO. The parent compound LaFeAsO exhibits a complex temperature dependence, consistent with the previous report.[22] S is negative over the entire temperature range, suggesting dominant electron-type conduction. The steep upturn just below 155 K is associated with the structural phase transition. Upon Co doping to x
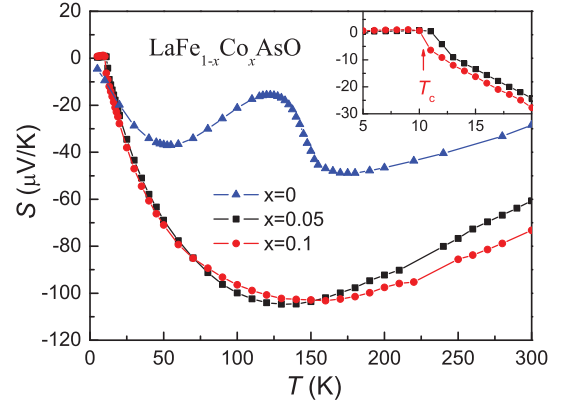
$= 0.05$ and 0.1, the upturn of S disappears, and the room-temperature $|S|$ values increase from 28 to ~ 70 $\mu V / K$. Band calculations[10] indicate multiband feature at Fermi level, leading to the electrical transport from both electrons and holes. Considering two bands with electron and hole conduction, respectively, for simplification, we have

$$S = \frac{\sigma_h |S_h| - \sigma_e |S_e|}{\sigma_h + \sigma_e}, \qquad (1)$$

where $\sigma_{h(e)}$ and $|S_{h(e)}|$ represent the contributions from holes (electrons) to the conductivity and thermopower, respectively. Therefore, the relatively small S value for the parent compound is, to some extent, due to the compensation effect of electron and hole conductions. With electron doping, the hole contribution in Eq. (1) becomes even smaller, explaining the increase in $|S|$ by the Co doping. In other words, our thermopower measurement suggests that electrons are indeed doped via the Co/Fe substitution.

It is noted that the Co valence in the end member LaCoAsO is 2+.[2,25] Therefore, one expects that the Co valence in LaFe$_{1-x}$Co$_x$AsO keeps the same value. Then, the realization of doping electrons by Co/Fe substitution is probably due to the itinerant character of Co 3d electrons. Such electron-doping mechanism of Co^{3+} for Fe^{2+} is unlikely. In fact, we prepared several "LaFe$_{1-x}$In$_x$AsO" samples. The result showed that In^{3+} (analogous to Co^{3+}) could not be doped into the lattice.

Figure 11 shows the temperature dependence of normal-state thermopower for SmFe$_{1-x}$Co$_x$AsO samples. Again, all of the thermopowers are negative in the whole temperature range, which means that the electronlike charge carriers dominate. For the undoped parent compound, thermopower starts to increase abnormally around T_{anom} at which the resistivity starts to decrease. This is similar to cases of LaFeAsO and TbFeAsO.[31] Such a remarkable change in the thermopower should be caused by the change in the electronic state when the system undergoes the structural phase transition and SDW transition. This anomaly is gradually suppressed with increasing Co doping and disappears for $x > 0.05$, consistent with the resistivity data. For the supercon-
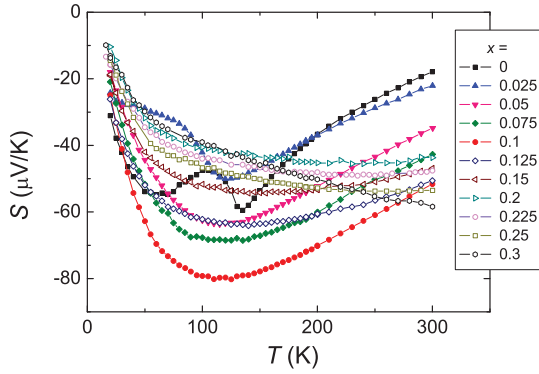
FIG. 11. (Color online) Temperature dependence of thermopower (S) for $SmFe_{1-x}Co_xAsO$ samples.

FIG. 12. (Color online) Doping dependence of room-temperature thermopower, $S(300)$, for $SmFe_{1-x}Co_xAsO$ samples. The superconducting transition temperature T_c^{mid} is also shown for comparison. The dashed line indicates the background term to the thermopower. $S'(300 \text{ K})$ is the abnormally enhanced term, equal to $S(300 \text{ K})$ subtracting the background normal term. See text for details.

ducting samples, the profile of $S(T)$ curves is very similar to that of high-T_c cuprates except that it is negative for $SmFe_{1-x}Co_xAsO$ system. However, in contrast to high-T_c cuprates where the value of normal-state thermopower decreases monotonously with increasing doping level,[32,33] the absolute value of thermopower, $|S|$, increases quickly with Co doping, and the maximum in $|S|$ is about 80 $\mu V/K$ for optimally doped level ($x=0.1$). Such a large value of $|S|$ is very unusual in superconducting materials. However, the remarkable enhancement of $|S|$ has also been observed in F-doped $LaFeAsO_{1-x}F_x$ (Refs. 22, 34, and 35) and in Th doped $Tb_{1-x}Th_xFeAsO$.[31] A rough estimate of $|S|$ according to the Mott expression gives a value of less than 10 $\mu V/K$ for F-doped $LaFeAsO$.[34] Whether the enhanced thermopower is associated with strong electron correlation, magnetic fluctuations, or specific electronic structure is an open issue.

It is well established that there is a universal doping (hole concentration) dependence of superconducting transition temperature, T_c, for high-T_c cuprates. Furthermore, it has been found that there exists a close correlation between the room-temperature thermopower, $S(290 \text{ K})$, and the hole concentration, p, and thus a universal correlation between T_c and $S(290 \text{ K})$ is observed.[32,33] In order to explore the possible relationship between thermopower and superconducting transition temperature in this system, we also plot both $S(300 \text{ K})$ and T_c^{mid} versus the doping level (x) for $SmFe_{1-x}Co_xAsO$ system. It becomes obvious that $S(300 \text{ K})$ increases with x as T_c^{mid} does for $x<0.1$, reaches a maximum at $x=0.1$, and then gradually decreases with x in the overdoped region. For $x>0.2$, superconductivity disappears and the thermopower starts to increase again. Actually it can be seen from Fig. 12 that there seem to be two different contributions to the thermopower; i.e., $S(300 \text{ K})=S_0(300 \text{ K})$ $+S'(300 \text{ K})$. The first term $S_0(300 \text{ K})$ is the normal contribution (shown by the dashed line in the superconducting window), which increases gradually with increasing x. The other term $S'(300 \text{ K})$ only appears in the superconducting window (shown by the blue open symbols in Fig. 12), which shows a domelike doping dependence as T_c^{mid} does. We propose that there should be a close correlation between superconducting state and the anomalous term $S'(300 \text{ K})$. It will be an interesting issue whether such a correlation between T_c and $S'(300 \text{ K})$ is a universal feature for all the iron-based arsenide superconductors.
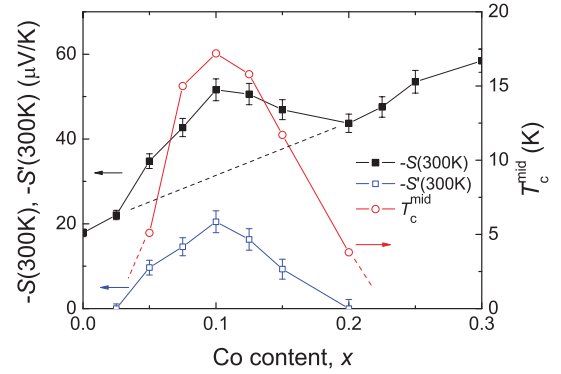
The anomalous contribution to the thermopower, represented by $|S'|(300 \text{ K})$, is hard to understand in the frame of a conventional metal. We note that the thermopower of a cobaltate Na_xCoO_2 is remarkably enhanced due to the electronic spin entropy.[36] Thus we suggest that the anomalous thermopower term might have a magnetic origin. Careful studies on the dc magnetic susceptibility have found that the normal-state magnetic susceptibility shows indeed a dome-like doping dependence in F-doped $LaFeAsO_{1-x}F_x$ system.[23] This susceptibility enhancement could be associated with spin fluctuations. Therefore it was proposed that the spin fluctuations may play an important role in the superconducting mechanism. However, the iron arsenide system has a very different nature in the electronic state compared to the sodium cobaltate system. In sodium cobaltate system, a strong electron correlation picture is necessary to describe electronic transport properties. The observation of suppression of thermopower by magnetic field suggested a large spin entropy term in thermopower. In contrast, the parent compounds $LnFeAsO$ in the iron arsenide system are not Mott insulators, and band calculations[10–13] and transport property measurements have suggested that the $3d$ electrons in this system have mainly itinerant nature. Therefore, the enhanced thermopower might not originate from the spin entropy, although we argue that it might have a magnetic origin. How the spin fluctuations play an important role in the electronic transport needs further studying. If both the enhanced thermopower and the enhanced susceptibility in the superconducting window have indeed the common origin, the magnetic fluctuations should also play an important role in the mechanism of superconductivity.

IV. CONCLUDING REMARKS

In summary, our systematic investigations on the transport, magnetic, and thermoelectric properties have established the electronic phase diagrams of cobalt-doped

LFe$_{1-x}$Co$_x$AsO (L=La and Sm) systems. Thermopower measurements indicate that conduction electrons are added with the cobalt doping, suggesting the itinerant nature of Co 3d electrons. The normal-state resistivity exhibits semiconductinglike behavior, making the Co-doped superconductors different from the F-doped ones. Furthermore, we found an anomalously enhanced thermopower in the superconducting region, which may be associated with the mechanism of superconductivity.

Co-doping-induced superconductivity challenges our previous understanding about the exploration of superconductivity via chemical doping. Conventionally, the dopants were nonmagnetic because magnetic atoms generally break superconducting Cooper pairs.[37] In addition, the doping site was mostly out of the superconducting structural unit, avoiding disorder effect. Representative examples include the Ba-doped La$_2$CuO$_4$,[38] K-doped BaBiO$_3$,[39] K-doped C$_{60}$,[40] and F-doped LaFeAsO.[1] In the present Co-doped LnFeAsO systems, however, the magnetic element cobalt does not act as superconducting Cooper-pair breakers. Additionally, superconductivity is robust in spite of significant doping (over 10 at. %) on the Fe$_2$As$_2$ conducting layers. These facts support the itinerant scenario of the Fe/Co 3d electrons, reminiscent of superconductivity on the border of itinerant-electron ferromagnetism in UGe$_2$.[41] For the cuprate superconductors, in sharp contrast, substitution of Cu with its neighbors in the Periodic Table (Ni and Zn) in CuO$_2$ plane severely destroys the superconductivity.[42] Therefore, our result suggests essential differences between the two classes of high-temperature superconductivity.

*ghcao@zju.edu.cn

†zhuan@zju.edu.cn

[1] Y. Kamihara, T. Watanabe, M. Hirano, and H. Hosono, J. Am. Chem. Soc. **130**, 3296 (2008).

[2] P. Quebe, L. J. Terbuchte, and W. Jeitschko, J. Alloys Compd. **302**, 70 (2000).

[3] X. H. Chen, T. Wu, G. Wu, R. H. Liu, H. Chen, and D. F. Fang, Nature (London) **453**, 761 (2008).

[4] G. F. Chen, Z. Li, D. Wu, G. Li, W. Z. Hu, J. Dong, P. Zheng, J. L. Luo, and N. L. Wang, Phys. Rev. Lett. **100**, 247002 (2008).

[5] Z. A. Ren, W. Lu, J. Yang, W. Yi, X. L. Shen, Z. C. Li, G. C. Che, X. L. Dong, L. L. Sun, F. Zhou, and Z. X. Zhao, Chin. Phys. Lett. **25**, 2215 (2008).

[6] Z. A. Ren, J. Yang, W. Lu, W. Yi, X. L. Shen, Z. C. Li, G. C. Che, X. L. Dong, L. L. Sun, F. Zhou, and Z. X. Zhao, Europhys. Lett. **83**, 17002 (2008).

[7] H. Kito, H. Eisaki, and A. Iyo, J. Phys. Soc. Jpn. **77**, 063707 (2008).

[8] C. Wang, L. J. Li, S. Chi, Z. W. Zhu, Z. Ren, Y. K. Li, Y. T. Wang, X. Lin, Y. K. Luo, S. Jiang, X. F. Xu, G. H. Cao, and Z. A. Xu, Europhys. Lett. **83**, 67006 (2008).

[9] R. J. Cava, J. Am. Ceram. Soc. **83**, 5 (2000).

[10] D. J. Singh and M.-H. Du, Phys. Rev. Lett. **100**, 237003 (2008).

[11] J. Dong, H. J. Zhang, G. Xu, Z. Li, G. Li, W. Z. Hu, D. Wu, G. F. Chen, X. Dai, J. L. Luo, Z. Fang, and N. L. Wang, Europhys. Lett. **83**, 27006 (2008).

[12] V. Cvetkovic and Z. Tesanovic, arXiv:0804.4678 (unpublished).

[13] G. Xu, W. Ming, Y. Yao, X. Dai, S.-C. Zhang, and Z. Fang, Europhys. Lett. **82**, 67002 (2008).

[14] A. S. Sefat, A. Huq, M. A. McGuire, R. Y. Jin, B. C. Sales, D. Mandrus, L. M. D. Cranswick, P. W. Stephens, and K. H. Stone, Phys. Rev. B **78**, 104505 (2008).

[15] During preparation of the manuscript on LaFe$_{1-x}$Co$_x$O [arXiv:0807.1304 (unpublished)], we became aware of an independent work of Sefat *et al.* (Ref. [14]) Our work on SmFe$_{1-x}$Co$_x$AsO was subsequently submitted [arXiv:0808.3254 (unpublished)]. Qi *et al.* (Ref. [16]) reported superconductivity in SmFe$_{1-x}$Co$_x$AsO in which only two Co-doped samples (x =0.10,0.15) were investigated.

[16] Y. Qi, Z. Gao, L. Wang, D. Wang, X. Zhang, and Y. Ma, Supercond. Sci. Technol. **21**, 115016 (2008).

[17] L. B. McCusker, R. B. Von Dreele, D. E. Cox, D. Louer, and P. Scardi, J. Appl. Crystallogr. **32**, 36 (1999).

[18] G. Wu, H. Chen, Y. L. Xie, Y. J. Yan, T. Wu, R. H. Liu, X. F. Wang, D. F. Fang, J. J. Ying, and X. H. Chen, Phys. Rev. B **78**, 092503 (2008).

[19] Jun Zhao, Q. Huang, Clarina de la Cruz, Shiliang Li, J. W. Lynn, Y. Chen, M. A. Green, G. F. Chen, G. Li, Z. Li, J. L. Luo, N. L. Wang, and Pengcheng Dai, Nature Mater. **7**, 953 (2008).

[20] C. H. Lee, A. Iyo, H. Eisaki, H. Kito, M. T. Fernandez-Diaz, T. Ito, K. Kihou, H. Matsuhata, M. Braden, and K. Yamada, J. Phys. Soc. Jpn. **77**, 083704 (2008).

[21] C. de la Cruz, Q. Huang, J. W. Lynn, J. Li, W. Ratcliff II, H. A. Mook, G. F. Chen, J. L. Luo, N. L. Wang, and P. Dai, Nature (London) **453**, 899 (2008).

[22] M. A. McGuire, A. D. Christianson, A. S. Sefat, B. C. Sales, M. D. Lumsden, R. Jin, E. A. Payzant, D. Mandrus, Y. Luan, V. Keppens, V. Varadarajan, J. W. Brill, R. P. Hermann, M. T. Sougrati, F. Grandjean, and G. J. Long, Phys. Rev. B **78**, 094517 (2008).

[23] T. Nomura, S. W. Kim, Y. Kamihara, M. Hirano, P. V. Sushko, K. Kato, M. Takata, A. L. Shluger, and H. Hosono, Supercond. Sci. Technol. **21**, 125028 (2008).

[24] C. Fang, H. Yao, W. F. Tsai, J. P. Hu, and S. A. Kivelson, Phys. Rev. B **77**, 224509 (2008).

[25] H. Yanagi, R. Kawamura, T. Kamiya, Y. Kamihara, M. Hirano, T. Nakamura, H. Osawa, and H. Hosono, Phys. Rev. B **77**, 224431 (2008).

[26] H. Luetkens, H.-H. Klauss, M. Kraken, F. J. Litterst, T. Dellmann, R. Klingeler, C. Hess, R. Khasanov, A. Amato, C. Baines, J. Hamann-Borrero, N. Leps, A. Kondrat, G. Behr, J. Werner, and B. Buechner, arXiv:0806.3533 (unpublished).

[27] T. Yildirim, Phys. Rev. Lett. **101**, 057010 (2008).

[28] Q. Si and E. Abrahams, Phys. Rev. Lett. **101**, 076401 (2008).

[29] F. Ma, Z. Y. Lu, and T. Xiang, Phys. Rev. B **78**, 224517 (2008).

[30] C. Zener, Phys. Rev. **82**, 403 (1951).

[31] L. J. Li, Y. K. Li, Z. Ren, Y. K. Luo, X. Lin, M. He, Q. Tao, Z. W. Zhu, G. H. Cao, and Z. A. Xu, Phys. Rev. B **78**, 132506 (2008).

[32] S. D. Obertelli, J. R. Cooper, and J. L. Tallon, Phys. Rev. B **46**, 14928 (1992).

[33] J. L. Tallon, C. Bernhard, H. Shaked, R. L. Hitterman, and J. D. Jorgensen, Phys. Rev. B **51**, 12911 (1995).

[34] A. S. Sefat, M. A. McGuire, B. C. Sales, R. Jin, J. Y. Howe, and D. Mandrus, Phys. Rev. B **77**, 174503 (2008).

[35] L. Pinsard-Gaudart, D. Berardan, J. Bobroff, and N. Dragoe, Phys. Status Solidi (RRL) **2**, 185 (2008).

[36] Y. Wang, N. S. Rogado, R. J. Cava, and N. P. Ong, Nature (London) **423**, 425 (2003).

[37] A. A. Abrikosov and L. P. Gorkov, Sov. Phys. JETP **12**, 1243 (1961); Zh. Eksp, Teor. Mat. Fiz. **39**, 1781 (1960).

[38] J. G. Bednorz and K. A. Muller, Z. Phys. B: Condens. Matter **64**, 189 (1986).

[39] R. J. Cava, B. Batlogg, J. J. Krajewski, R. Farrow, L. W. Rupp, A. E. White, K. Short, W. F. Peck, and T. Kometani, Nature (London) **332**, 814 (1988).

[40] A. F. Hebard, M. J. Rosseinsky, R. C. Haddon, D. W. Murphy, S. H. Glarum, T. T. M. Palstra, A. P. Ramirez, and A. R. Kortan, Nature (London) **350**, 600 (1991).

[41] S. S. Saxena, P. Agarwal, K. Ahilan, F. M. Grosche, R. K. W. Haselwimmer, M. J. Steiner, E. Pugh, I. R. Walker, S. R. Julian, P. Monthoux, G. G. Lonzarich, A. Huxley, I. Sheikin, D. Braithwaite, and J. Flouquet, Nature (London) **406**, 587 (2000).

[42] J. M. Tarascon, L. H. Greene, P. Barboux, W. R. McKinnon, G. W. Hull, T. P. Orlando, K. A. Delin, S. Foner, and E. J. McNiff, Phys. Rev. B **36**, 8393 (1987).